# Titin force enhancement following active stretch of skinned skeletal muscle fibres

Krysta Powers[1], Venus Joumaa[1], Azim Jinha[1], Eng Kuan Moo[1], Ian Curtis Smith[1],

Kiisa Nishikawa[2] & Walter Herzog[1]

Human Performance Laboratory, Department of Kinesiology, University of Calgary[1]

Human Performance Laboratory, KNB 404

2500 University Dr. NW

Calgary, AB Canada T2N 1N4

Department of Biological Sciences, Northern Arizona University[2]

617 S. Beaver Street, Biological Sciences (Building 21)

Flagstaff, AZ USA 86001

**Corresponding Author**: Krysta Powers

klpowers@ucalgary.ca

## SUMMARY STATEMENT

Titin force is differentially enhanced in skinned skeletal muscle fibres from control and titin-mutant mice.


## ABSTRACT

In actively stretched skeletal muscle sarcomeres, titin-based force is enhanced, increasing the stiffness of active sarcomeres. Titin force enhancement in sarcomeres is vastly reduced in *mdm*, a genetic mutation with a deletion in titin. Whether loss of titin force enhancement is associated with compensatory mechanisms at higher structural levels of organization, such as single fibres or entire muscles, is unclear. The aim of this study was to determine whether mechanical deficiencies in titin force enhancement are also observed at the fibre level, and whether mechanisms compensate for the loss of titin force enhancement. Single skinned fibres from control and mutant mice were stretched actively and passively beyond filament overlap to observe titin-based force. Mutant fibres generated lower contractile stress (force divided by cross-sectional area) than control fibres. Titin force enhancement was observed in control fibres stretched beyond filament overlap, but was overshadowed in mutant fibres by an abundance of collagen and high variability in mechanics. However, titin force enhancement could be measured in all control fibers and most mutant fibres following short stretches, accounting for ~25% of the total stress following active stretch. Our results show that the partial loss of titin force enhancement in myofibrils is not preserved in all mutant fibres and this mutation likely affects fibres differentially within a muscle. An increase in collagen helps to reestablish total force at long sarcomere lengths with the loss in titin force enhancement in some mutant fibres, increasing the overall strength of mutant fibres.


Journal of Experimental Biology • Advance article

## INTRODUCTION

The most basic contractile unit of a skeletal muscle is the sarcomere; a semi-crystalline structure composed of proteins that generate the force required for movement. Sarcomeres are linked in series to form myofibrils, and are joined in parallel to comprise a single, multinucleated muscle fibre (Fig. 1). Each sarcomere is made up of three main filaments that contribute to sarcomere force: thick filaments, thin filaments and titin (Fig. 1). The force generated by calcium-activated sarcomeres has been described traditionally by cross-bridge cycling between the thick and thin filaments (Rayment et al., 1993). Nevertheless, active sarcomeres are routinely stretched during movement and generate more force following stretch than can be explained by cross-bridges alone (Herzog and Leonard, 2002). Because this additional force depends on the magnitude but not the speed of stretch, and because it results in increased passive force (passive residual force enhancement), it has been speculated that titin contributes to this unexplained extra force (Herzog and Leonard, 2002; Leonard and Herzog, 2010; Nishikawa et al., 2012; Powers et al., 2014, 2016).

Titin contributes 95-98% of the passive force in sarcomeres and myofibrils (Bartoo et al., 1997; Wang et al., 1993); resisting sarcomere lengthening by elongation of serial springs along its free length (Linke et al. 1998; Granzier and Labeit, 2004). While titin was not traditionally considered a contributor to the force of active sarcomeres, this view is now challenged by observations demonstrating that titin force increases during activation (Bianco et al., 2007; Campbell and Moss, 2002; Kellermayer and Granzier, 1996; Labeit et al., 2003; Leonard and Herzog, 2010; Linke et al., 2002; Nagy et al., 2004; Tatsumi et al., 2001). Enhanced force of a passive element in actively stretched sarcomeres was suggested nearly 40 years ago by Edman et al. (1978), but was not observed until 2002 (Herzog and Leonard, 2002). These initial observations of ‘passive force enhancement’ demonstrated that, following active stretch, titin-based force remained greater after deactivation than its passive force at corresponding lengths in cat soleus muscle (Herzog and Leonard, 2002). Titin force enhancement was investigated in rabbit (and later, mouse) psoas myofibrils stretched actively beyond filament overlap (Leonard and Herzog, 2010; Powers et al., 2014). These studies showed a 400% increase in titin-based force in sarcomeres stretched actively to 6.0 μm, when compared to titin-based force in sarcomeres passively stretched to the same length, greatly exceeding the 20% increase in titin force previously measured following deactivation of actively stretched myofibrils (Joumaa et al., 2008).

The molecular details of how titin-based force is enhanced in an active sarcomere remain unclear. It is well established that titin becomes stiffer in the presence of calcium (DuVall et al., 2013; Labeit et al., 2003). However, the calcium-based increase in titin force in intact sarcomeres is too small to explain the force increase after actively stretch (Joumaa et al., 2008; Powers et al., 2014). Early investigations demonstrated that the magnitude of titin force enhancement depends on sarcomere length at activation; titin force enhancement increases with increased initial contractile force, suggesting that titin-based force is proportional to cross-bridge force (Leonard and Herzog, 2010). Subsequent studies showed effective suppression of titin force enhancement when cross-bridge force is chemically inhibited (Joumaa et al., 2008; Labeit et al., 2003; Powers et al., 2014), suggesting that the titin force enhancement mechanism may become engaged by the onset of cross-bridge cycling or at a threshold of contractile force production.

A titin gene mutation in mice, *muscular dystrophy with myositis* (Garvey et al., 2002), may be a powerful tool to further pursue the mechanism(s) governing titin force enhancement due to the deletion of potentially crucial force regulation sites on titin (Fig. 1). In a recent study, we showed that modulation of titin force results in a stiffer titin in mouse psoas myofibrils compared to passively stretched myofibrils (Powers et al., 2014). However, no increase in the stiffness of titin was observed in mutant sarcomeres, suggesting that titin-based force regulatory mechanisms are affected by the *muscular dystrophy with myositis (mdm)* mutation (Powers et al., 2016). Investigations of whole *mdm* soleus have also demonstrated active compliance of mutant soleus muscles in comparison to wildtype controls (Monroy et al., 2016; Taylor-Burt et al., 2015), further supporting the idea that titin-based force regulation is affected by the *mdm* mutation. From this work, we speculate that force regulatory sites are deleted from *mdm* titin.

*Muscular dystrophy with myositis* is characterized by a mutation in the *Ttn* gene (Garvey et al., 2002), resulting in (what is predicted to be) an 83 amino acid deletion in the N2A-PEVK region of the titin protein (Garvey et al., 2002). Due to the large size of the titin protein, gel analyses are not sensitive enough to detect any change in size of *mdm* titin (Garvey et al., 2002), which may be missing more amino acids than predicted due to aberrant post-translational processing (Lopez et al., 2008; Buck et al., 2014). M*dm* mice are smaller than wild type mice, exhibit an abnormal gait, have disrupted thermoregulation and die prematurely (Garvey et al., 2002; Huebsch et al., 2005; Monroy et al., 2016; Taylor-Burt et al., 2015). *Mdm* mutant muscles show muscle and fibre atrophy (Huebsch et al., 2005; Lopez et al., 2008;

Monroy et al., 2016; Taylor-Burt et al., 2015), increased satellite cell populations (Heimann et al., 1996), increased occurrence of centralized nuclei (Heimann et al., 1996; Lopez et al., 2008), and large connective tissue deposits (Lopez et al., 2008). At the myofibril level, mutant sarcomeres are indistinguishable from healthy controls (Powers et al., 2016; Witt et al., 2004), suggesting that the *mdm* mutation does not affect the structure of the sarcomeres. Nevertheless, mechanical studies show decreased contractile force and increased passive force in *mdm* muscles (Huebsch et al., 2005; Lopez et al., 2008; Monroy et al., 2016; Taylor-Burt et al., 2015), suggesting that the deletion in titin and subsequent loss of titin force enhancement may influence the contractile mechanics of *mdm* muscles.

The predicted deletion in *mdm* titin results in a partial deletion of a calpain-3 (CAPN3) binding domain in N2A titin (Garvey et al., 2002; Huebsch et al., 2005; Witt et al., 2004), resulting in decreased CAPN3 levels in mutant soleus muscles (Huebsch et al., 2005). The role of CAPN3 in skeletal muscle is diverse, with contributions to numerous cellular processes, such as apoptosis, myogenesis, sarcomere formation and calcium release (Kramerova et al., 2008). Thus, it was initially thought that altered signaling may explain the *mdm* phenotype (Witt et al., 2004) However, after a comprehensive investigation of the physiological effects of CAPN3 on complex motor behavior in *mdm* mice, (Huebsch et al., 2005) concluded that neither a reduction in CAPN3, nor its irregular activity is responsible for initiation or progression of *mdm* muscular dystrophy. Further investigations of signaling-based disruptions in N2A titin showed that select muscle ankryin repeat proteins (MARPs) are up-regulated in *mdm* mutant soleus muscle (Witt et al., 2004). MARPs bind to the N2A segment of titin and have been speculated to act as the molecular links between myofibrillar stretch-induced signaling and muscle gene expression (Miller et al., 2003). Since MARPs and CAPN3 bind in close proximity on titin, one proposed function of N2A titin is to coordinate MARP and CAPN3 signaling pathways during imposed mechanical stress on the sarcomeres (Miller et al., 2003). It is possible that disruptions in normal N2A signaling from the *mdm* mutation contribute to altered force regulation in the mutated titin protein, however, this possibility remains relatively unexplored.

We recently showed that *mdm* mutant psoas myofibrils generate reduced contractile force and exhibit active compliance, however, in contrast to whole muscle studies, passive force was not affected by the deletion in titin (Powers et al., 2016). The inherent passive properties of titin remain unchanged in mutant psoas myofibrils, suggesting that any increase in passive force in *mdm* mutant muscle (and any change in the structure of mutant muscle) is

due to secondary effects of the mutation. The mechanical properties of titin were, however, altered in actively stretched mutant myofibrils, as the majority of titin force enhancement was abolished with the *mdm* deletion in titin. This brought us to question whether the loss of titin force enhancement at the sarcomere level translates into deficient muscle function seen in *mdm* mutant mice. Titin force enhancement has only been observed in a myofibril preparation and it is unclear how a loss of titin force enhancement would influence higher levels of structural organization in muscle.

Thus, the aim of this study was to determine whether mechanical deficiencies in titin force enhancement are observed at the fibre level in *mdm* mutant psoas muscle, and if so, whether other mechanisms compensate for the loss of titin force enhancement. We hypothesized that mutant psoas fibres would generate reduced contractile force and reduced titin force enhancement, corresponding directly to the mechanical observations previously made in single myofibrils.

## MATERIALS AND METHODS

### *Ethics and Animals*

Tissue from *muscular dystrophy with myositis* (*mdm*) mouse psoas was obtained from a colony established at Northern Arizona University's Animal Care Facility (Flagstaff, AZ, USA) using breeding pairs of B6C3Fe a-/a-*mdm* mice from the Jackson Laboratory (Bar Harbor, ME, USA). Homozygous recessive $Ttn^{mdm}$ (mutant) mice were confirmed by genotyping (Lopez et al., 2008) and sacrificed at 27-41 days for experiments. Age matched wild type C57-BL/6 mice from the University of Calgary were used as a healthy comparison (control) group. Ethics approval for this study was granted by the Life and Environmental Sciences Animal Ethics Committee of the University of Calgary and the Institutional Animal Care and Use Committee at Northern Arizona University.

### *Skinned fibre preparation*

A skinned fibre preparation was used in an attempt to limit endomysial contributions to passive tension. Strips of psoas muscle were dissected from euthanized animals, tied to small wooden sticks, and stored in a relaxing solution *(in mM)*: potassium propionate (170), magnesium acetate (2.5), MOPS (20), $K_2$EGTA (5) and ATP (2.5), pH 7.0, for 12 hours at 4ºC, then in a relaxing-glycerol (50:50) solution at -20ºC for four to six weeks. All solutions used

in this study contained one tablet of protease inhibitor (Complete, Roche Diagnostics, Quebec, Canada) per 100 ml of solution.

On the day of the experiments, a single fibre was dissected from the skinned muscle biopsy and transferred to an experimental glass chamber containing relaxing solution. One end of the fibre was glued to the hook of a length controller and the other end to the hook of a force transducer (Aurora Scientific Inc., Model 400A, Ontario, Canada), allowing for control of fibre length and measurement of force, respectively. Sarcomere length was measured using optical diffraction of a He-Ne laser beam. When sarcomere length was measurable in mutant fibres, a sarcomere length of 2.5 μm was reached when fibres were straightened from their visual slack. Sarcomere length could not be measured in ~80% of mutant fibres because a first order diffraction pattern was not visible. Thus, in mutant fibres where sarcomere length could not be measured, fibres were straightened until no visual slack remained.

The diameter of each fibre was measured using a binocular dissecting microscope at a magnification of ×5. Cross-sectional area was calculated assuming a cylindrical shape. Force was normalized relative to cross-sectional area.

*Mechanical Tests*

Prior to mechanical tests, fibres were carefully examined for damage incurred during preparation. Fibres with any visible damage were excluded from the study. Fibres were first tested for viability. Each mutant and control fibre was adjusted to an initial sarcomere length of 2.5 μm ($L_0$) in relaxing solution and then switched to a washing solution *(in mM)*: potassium propionate (185), magnesium acetate (2.5), MOPS (20) and ATP (2.5), pH 7.0. Fibres were activated by exchanging washing solution for calcium-activating solution *(in mM)*: potassium propionate (170), magnesium acetate (2.5), MOPS (10), ATP (2.5) and CaEGTA/$K_2$EGTA mixed at different proportions to obtain a pCa (-log [$Ca^{2+}$]) of 4.2, pH 7.0. Steady state force was measured after 15 seconds of stress relaxation as an average of 200 data points. The change in force, normalized to fibre cross sectional area, is reported as 'contractile stress' ($mN/mm^2$). Analysis was completed using a custom Matlab program.

For initial investigation of titin force enhancement, viable mutant and control fibres were randomly distributed into 'passive' and 'active' conditions. Fibres in both groups were stretched from $L_0$ to final average sarcomere lengths of 5.2 μm, far exceeding filament overlap (*long stretch* groups). Fibres were stretched to very long lengths in order to observe any increase in titin-based force in actively stretched fibres. This magnitude of stretch, while not

physiologically relevant, is necessary for measurement of titin force in the absence of cross-bridges. Fibres were stretched at a speed of 21.6% of the fibre length/second and held isometrically to reach a steady state force (at an average sarcomere length of 5.2 μm). Fibres in the "passive" group were stretched in relaxing solution (Fig. 2A) while fibres in the "active" group were stretched in calcium-activating solution (Figure 2B). For these long stretches, titin force enhancement was determined to be the percent increase in average steady state active stress from the average passive steady state stress. Each fibre was only stretched in one condition (active or passive) due to the likelihood of incurring damage with the magnitude of stretch.

An independent group of skinned fibres underwent a short passive and active stretch protocol to allow for comparison of titin force enhancement in individual fibres. Single skinned fibres were adjusted to $L_0$ (sarcomere length 2.5 μm) using the methods described above. Fibres were passively stretched (in relaxing solution) by 28% of $L_0$ at a speed of 21.6% of the fibre length/second and held isometrically to reach a steady state force (at an average sarcomere length of 3.2 μm) before being shortened back to $L_0$. Fibres were then activated using the protocol described above, allowed to reach a contractile steady-state force, and actively stretched 28% of $L_0$ at a speed of 21.6% of the fibre length/second and held isometrically to reach a steady state force at an average sarcomere length of 3.2 μm. Contractile stress at 3.2 μm was calculated for each fibre using the measured contractile force at 2.5 μm and assuming a linear relationship force-length relationship that approaches zero at a sarcomere length of 4.0 μm.

At 3.2 μm sarcomere lengths, cross-bridges and passive forces contribute to the total force of a fibre. Thus, at 3.2 μm, titin force enhancement ($mN/mm^2$) was determined to be the stress remaining after subtracting a fibre's passive stress and contractile stress at 3.2 μm. The percent (%) titin force enhancement was calculated as a percentage of the total stress following active stretch to 3.2 μm.

For all mechanical experiments, fibres that did not generate measurable contractile force during the initial activation or exhibited decreases in force during stretch were considered damaged and excluded from analyses. All mechanical tests were conducted using room temperature solutions (~21°C).

*Fibre Imaging*

Fibres from control (n = 50) and mutant (n = 38) skinned psoas biopsies were isolated and imaged using an inverted light microscope (Zeiss Axiovert 200M) under 40 and ×100 oil immersion to compare fibre diameter and morphology. Second harmonic generation imaging techniques were used to visualize the fibre striation pattern in mutant (n = 9) and control (n = 4) fibres (Moo et al., 2016), isolated from a single mutant and control psoas muscle. Two photon excitation imaging techniques were used to visualize the nuclei of the fibres. A laser wavelength of 800 nm was used. The resulting second harmonic generation and two photon excitation signals were collected in the backward (epi-) direction using two separate band-pass filters at the harmonic frequency (FF01 400/40, Semrock Inc. NY, USA) and at ~510 nm (FF01 520/70, Semrock Inc. NY, USA), respectively.

Fibres were isolated and placed on a microscope slide. The nuclei of the muscle fibres were positively stained at room temperature (21°C) with Syto 13 (5 µM; excitation$_{max}$: 488nm; emission$_{max}$: 509; Molecular Probe, OR, USA) for 30 minutes. After staining, samples were washed in dye-free phosphate buffered saline. Muscle fibres were imaged using an upright, multi-photon excitation microscope (FVMPE-RS model, Olympus, Tokyo, Japan) equipped with a wavelength-tunable (680 – 1300 nm), ultrashort-pulsed laser (pulse width: <120 fs; repetition rate: 80 MHz; InSight DeepSee-OL, Spectra-Physics, CA, USA) and a 25 x/1.05 NA water immersion objective (XLPLN25XWMP2 model, Olympus, Tokyo, Japan). A series of planar images was acquired in the horizontal plane (xy-plane) (imaging area: 159 µm x 159 µm; pixel size: 0.155 µm; bit-depth: 12; dwell time: 2 µs) along the objective axis (z-axis) that is perpendicular to the horizontal plane at 1 µm intervals. The average power in the sample plane was varied from 14 – 40 mW in order to produce optimal images.

*Collagen Analysis*

The mass of collagen in skinned fibres was evaluated using a colorimetric hydroxyproline (HYP) assay. Skinned fibres from control (n = 45) and mutant (n =30) psoas were isolated and hydrolyzed in vials containing 6M HCl (7 µl HCl per 1 µg of muscle tissue). The vials were incubated for 18 hours at 105°C then analyzed for HYP content using the Hydroxyproline Assay Kit (SIGMA-ALDRICH, MAK008). HYP concentration was determined by the reaction of oxidized HYP with 4-(Dimethylamino) benzaldehyde (DMAB), resulting in a colorimetric product (560 nm) proportional to the concentration of HYP present. Measured HYP mass (µg) was used to calculate approximate collagen mass using the equation:

collagen mass = 7.25 x measured mass of HYP (De Jaeger et al., 2015; Woessner, 1961). Collagen mass is expressed as a percentage (%) normalized to the mass of pooled control (n =6) and mutant (n = 5) skinned fibres.

*Statistics*

An independent samples t-test was used to compare steady state contractile stress (at 2.5 μm sarcomere length) in control and mutant fibres with a Levene's test for equality of variance. Kruskal-Wallis non-parametric statistics were used to compare steady state stress in active and passive mutant and control fibres following 108% stretch (5.2 μm sarcomere lengths). A pairwise comparison was used to identify differences between groups with a Bonferroni correction to account for multiple comparisons. Titin force enhancement in short stretches was compared using Mann-Whitney U non-parametric statistics. Spearman's rank order correlation was used to determine the correlation between contractile stress and titin force enhancement in fibres stretched to 3.2 μm sarcomere lengths. Kolmogorov-Smirnov tests were used to test for normal distribution of data in all conditions. Mann-Whitney U non-parametric statistics were used to compare collagen concentration in skinned mutant and control fibres. An alpha level of 0.05 was used to determine statistical significance.

**RESULTS**

*Morphology*

Mutant fibres are smaller in diameter (n, mean ± SD; 38, 19.9 μm ± 4.4) than control fibres (50, 52.3 μm ± 10.1) ($p < 0.05$) (Fig. 3). In addition to a 60% reduction in fibre diameter, some mutant fibres differed qualitatively in appearance from healthy fibres. Under the light microscope ~30% of mutant fibres express nuclei aligned along the center of the fibre (Fig. 3B). Staining for nuclei and subsequent second harmonic generation and two photon excitation imaging confirmed differential arrangements of nuclei and sarcomere arrangement in mutant compared to control fibres. A clear striation pattern was seen in all imaged control fibres, with multiple nuclei located on the periphery (Fig. 4). Mutant fibres were variable in appearance and nuclei arrangement. Only 5 of the 9 mutant fibres displayed a clear striation pattern with 2 fibres containing centralized nuclei (Fig. 4).

*Collagen Content*

Skinned mutant fibres (n, mean ± SD; 5, 7.9 ± 3.5%) contained a higher percentage of collagen than control fibres (6, 0.3 ± 0.1%; $p = 0.004$; Fig. 5).

*Mechanical Tests*

Steady state contractile stress of fibres activated at $L_0$ (2.5 μm) was lower in mutant (n, mean ± SD; 31, 81 mN/mm$^2$ ± 67) than control fibres (35, 115 mN/mm$^2$ ± 40) ($p$ = 0.017, Fig. 6). The variability of steady state contractile stress was greater in mutant than control fibres ($p$ = 0.049).

Steady state stress following stretch beyond filament overlap (108% $L_0$; average sarcomere length 5.2 μm) differed across genotypes and conditions ($p$ = 0.0003). A Bonferroni corrected p-value of 0.0083 was used to determine statistical significance following multiple comparisons. Steady state stress following active stretch did not differ between mutant (18, 205 ± 98 mN/mm$^2$) and control fibres (15, 152 ± 36 mN/mm$^2$; $p$ = 0.0596; Fig. 7). Steady state stress following passive stretch was higher in mutant (11, 226 ± 101 mN/mm$^2$) than control fibres (10, 90 ± 41 mN/mm$^2$; $p$ = 0.0009). Steady state active stress was greater than steady state passive stress in control fibres ($p$ = 0.0005). Steady state active and passive stress did not differ in mutant fibres ($p$ = 0.5872, Fig. 7).

For 5.2 μm stretches, titin force enhancement was calculated as the percent increase in stress from the mean passive steady state stress to the mean active steady state stress at the end of stretch (5.2 μm sarcomere lengths). Control fibres showed (mean ± SD; 69 ± 39%) titin force enhancement. Because there was no statistical increase between passive and active steady state stress in mutant fibres stretched beyond filament overlap (to 5.2 μm), there was no quantifiable titin force enhancement in mutant fibres stretched to 5.2 μm sarcomere lengths (Fig. 7).

In individual fibres stretched to 3.2 μm, titin force enhancement was defined as the stress remaining in an actively stretched fibre after subtracting the passive stress and contractile stress at average end sarcomere length of 3.2 μm. The percent titin force enhancement (of the total stress following active stress) did not differ between mutant 22 ± 18% (mean ± SD) and control fibres 28 ± 9% ($p$ = 0.557, *Mann-Whitney U*). Mutant fibres had higher variability in titin force enhancement than control fibres ($p$ = 0.011, *Levene's test*; Fig. 8). The variation in magnitudes of titin force enhancement (mN/mm$^2$) in fibres stretched to 3.2 μm was correlated with the contractile stress at $L_0$ (2.5 μm) in mutant ($p$ = 0.001, *Spearman's correlation coefficient* = 0.836) and control ($p$ = 0.005, *Spearman's correlation coefficient* = 0.806). Steady state contractile stress explained 65% of the variability in titin force enhancement in control fibres ($R^2$ = 0.649). Contractile stress explained 70% of the variability in titin force enhancement in mutant fibres ($R^2$ = 0.699) (Fig. 9).

## DISCUSSION

Titin force enhancement refers to the observation that the steady state force of sarcomeres stretched actively beyond filament overlap is greater than the steady state force of sarcomeres stretched passively to corresponding lengths. This increase in force from steady state passive to active states beyond filament overlap is inferred to come from modulation of titin-based force by a mechanism not yet understood. Current speculation is that titin force is modulated when the titin protein becomes shorter and stiffer upon activation (Herzog et al., 2016; Leonard and Herzog, 2010; Nishikawa et al., 2012; Schappacher-Tilp et al., 2015). Previous studies in myofibrils from *mdm* mice show that, with a deletion in the titin protein, titin force enhancement and contractile force are substantially decreased (Powers et al., 2016). Titin force modulation is thought to occur during contractile force production, therefore, this mechanism may have implications for understanding the mechanics of actively stretched skeletal muscle.

Until now, titin force enhancement had only been observed in myofibril preparations (Leonard and Herzog, 2010; Powers et al., 2014) in which titin force dominates at lengths beyond filament overlap (Bartoo et al., 1997; Wang et al., 1993). Thus, we sought to explore how deficiencies in titin force enhancement in myofibrils with a deletion in titin would present in a less-reduced, single fibre preparation. We hypothesized that titin force enhancement and contractile force would be decreased in mutant fibres, corresponding with previous results in myofibrils (Powers et al., 2016). We found that titin force enhancement was not measurable in mutant fibres stretched beyond filament overlap. However, in fibres stretched to 3.2 μm sarcomere lengths, titin force enhancement, determined to be the residual stress after subtracting out passive and contractile components, was measurable in most mutant fibres and did not differ, on average, from control fibres. Mutant fibres generated variable contractile stress that was, on average, lower than the contractile stress of control fibres activated at optimal filament overlap (Fig. 6).

Skinned mutant fibres are weaker on average than control fibres when activated at 2.5 μm sarcomere lengths (Fig. 6). This finding corroborates with myofibrils (Powers et al., 2016) and studies across variable muscle preparations showing that *mdm* mutant skeletal muscles generate less contractile force than controls (Huebsch et al., 2005; Lopez et al., 2008; Monroy et al., 2012; Taylor-Burt et al., 2015). However, skinned mutant psoas fibres show only a 30% reduction in the average contractile stress compared to control fibres. In mutant myofibrls, the reduction in contractile stress is more than 60% (Powers et al., 2016). Thus, skinned mutant

fibres are stronger than mutant myofibrils. In fibres, sarcomeres are strengthened by the stabilizing intermediate filament desmin, which also contributes to optimal generation and/or transmission of contractile force (Balogh et al., 2003). Partial recovery of contractile force may be facilitated by increased stabilization of sarcomeres by desmin and other intermediate filaments that are not present in a myofbril preparation. As well, an increase in collagen (Fig. 5) provides additional stability to skinned mutant fibres.

Another possible explanation for force recovery between myofibrils and fibres relates to the high variability of contractile stress in mutant fibres. Although normally distributed, the spread of mutant contractile stresses shows different populations of mutant fibres (Fig. 6); fibres that are weak and fibres that are strong. This idea is also supported by our imaging data (Fig.4) in which different mutant fibre morphologies were observed. A clear striation pattern was observed in all imaged control fibres (Fig. 4A), indicating regular arrangement of thick filaments and organization of myofibrils within fibres (Greenhalgh et al., 2007). However, in mutant fibres, a clear striation pattern was visible in only 5 of 9 fibres, suggesting that the semi-crystalline structure is disturbed in a subset of mutant fibres (Fig. 4B). The two "populations" of mutant fibres that were imaged included: (1) fibres with a clear striation pattern and multiple peripheral nuclei, which although smaller than control fibres, had no morphological features indicative of disease (Fig. 4B); and (2) fibres with an unclear striation pattern and centrally aligned nuclei (Figs 3B, 4C). Previous studies have reported a 20% increase in centralized nuclei in *mdm* mutant diaphragm and soleus muscles (Huebsch et al., 2005; Lopez et al., 2008), which is in agreement with the results found in the present study. These data demonstrate that a subset of mutant fibers are severely affected by the *mdm* mutation in titin. Since all imaged fibres came from the same mutant muscle, we conclude from these results that individual mutant fibres within a muscle are differentially affected by the *muscular dystrophy with myositis* mutation or that there is a time dependence to the mutation and we imaged fibres at different stages of degeneration.

We hypothesize that the mechanical properties of the mutant fibre populations differ greatly, with strong mutant fibers (Fig. 4B) mitigating some of the mechanical consequences of severely affected fibers (Fig. 4C). It can be inferred that the lack of a clear striation pattern in a subset of mutant fibres results from misalignment of sarcomeres within fibres, possibly due to the loss of contractility in *mdm* mutant myofibrils (Powers et al., 2016; Sparrow and Schöck, 2009). Since sarcomere morphology is normal in *mdm* mutant psoas (Powers et al., 2016), contractile force either cannot be sustained or is not properly transmitted from the sarcomere despite a normal appearance (Balogh et al., 2003). Thus, deficient contractile force

production in mutant psoas sarcomeres (Powers et al., 2016) may present morphologically as the misalignment of myofibrils in some mutant fibres while in other mutant fibres, the misalignment of sarcomeres is somehow mitigated. Desmin is also involved in the alignment of sarcomeres and myofibrils (Wang and Ramirez-Mitchell, 1983) within a fibre, as well as nuclear positioning (Palmisano et al., 2015). It is possible that functional disruptions in desmin contribute to misalignment of myofibrils in mutant fibres and to the central alignment of nuclei in some mutant fibres. Future studies of *muscular dystrophy with myositis* skeletal muscle should explore possible disturbances in desmin or other intermediate filaments that may occur with the *mdm* mutation.

Despite changes in morphology, when mutant fibres were actively stretched beyond filament overlap, the steady state stress did not differ from control fibres (Fig 7). While comparable in magnitude, the source of mutant and control force differed. The total force of mutant fibres stretched beyond filament overlap is entirely explained by the passive force of mutant fibres, whereas in control fibres, passive force cannot explain the total force following active stretch. The inherent passive stiffness of *mdm* titin is unaltered in mutant psoas (Powers et al., 2016), thus, we know that passive components other than titin increase the force of mutant fibres to achieve the same magnitude of force in actively stretched mutant and control fibres.

Passive tension in single fibres is thought to arise primarily from titin and collagen, with intermediate filaments contributing nominally at long sarcomere lengths (Granzier and Irving, 1995). In skinned mutant fibres, greater passive stress can be attributed to a substantial increase in collagen (Fig. 5). Fibrosis has been shown previously in *mdm* diaphragm, with collagen deposits specifically in the endomysium (Lopez et al., 2008). It is thought that during the skinning process, single fibres are chemically then mechanically removed from the surrounding endomysia (Meyer and Lieber, 2011) allowing skinned fibre experiments to mainly assess the mechanical properties of the contractile proteins and intermediate filaments (Eastwood et al., 1979). Skinned control fibres contain only 0.3% collagen (Fig. 5). However, the skinning process is less effective in removing endomyosial collagen from skinned mutant fibres, which are made up of almost 8% collagen. This excess in collagen may introduce a source of resistive force in skinned mutant fibres stretched beyond filament overlap. We were unable to detect collagen in control or mutant psoas skinned fibres using the second harmonic generation technique (Fig. 4), which indicates that the residual collagen is irregularly organized (Boerboom et al., 2007). From these results, we conclude that collagen increases the passive stress of actively and passively stretched skinned mutant fibres. This increase in collagen

increases the strength of mutant fibers, allowing for comparable magnitudes of active stress in control and mutant skinned fibres stretched beyond filament overlap.

Control fibers generate less passive stress than active stress following stretch beyond filament overlap; the total stress of actively stretched control fibers exceeds the passive component of stress (Fig. 6). However, there was no difference between the passive and active steady state stress of mutant fibers following stretch beyond filament overlap (Fig. 7). We initially speculated that the increase in active compared to passive steady state stress in control fibers stretched beyond filament overlap was due to engagement of the titin force enhancement mechanism, while no increase between passive and active steady state stress in mutant fibers indicates that the titin force enhancement mechanism is not engaged in mutant fibers. This finding would agree with results from mutant myofibrils, which show almost no titin force enhancement (Powers et al., 2016).

With the variability in morphology and mechanics across mutant fibres and the substantial increase in collagen, additional investigations were required to determine that the titin force enhancement mechanism is not engaged in mutant fibers. To further investigate titin force enhancement while taking into account the variability in mechanics across fibres and the influence of collagen at long sarcomere lengths, we calculated titin force enhancement in individual fibres that were passively and actively stretched to short sarcomere lengths (3.2 μm). Titin force enhancement was determined to be the residual stress after subtracting the contractile and passive stresses of each fibre at end length (3.2 μm), expressed as a percentage of the total stress at the end of active stretch. We acknowledge the possibility that this force enhancement following active stress within filament overlap may come from a variety of sources. Nevertheless, we presume that the extra force beyond passive and contractile components in the fibre result from modulation of titin based force that can be observed at the myofibril level. Titin force enhancement was measured in all control fibres, signifying an effective method for resolving titin force enhancement in fibres stretched within filament overlap. By eliminating the variability between mutant fibres, titin force enhancement was also measurable in mutant fibres. Titin force enhancement was variable across mutant and control fibres, with mutant fibres exhibiting higher variability than control fibres. Titin force enhancement did not differ between genotypes; contributing approximately 25% of the total stress at the end of active stretch to 3.2 μm. Titin force enhancement was only absent in 2 of 11 mutant fibres but was variable in the remaining 9 mutant fibres, with 3 mutant fibres generating more than 40% titin force enhancement and bringing up the average titin force

enhancement in mutant fibres (Fig. 8). The high variability in mutant titin force enhancement further supports our speculation of differential effects of the *mdm* mutation.

We previously observed that the magnitude of titin force enhancement in myofibrils depends on the contractile force prior to stretch (Leonard and Herzog, 2010; Powers et al., 2014). In the present study, we saw a strong correlation between contractile stress and the magnitude of titin force enhancement in fibres stretched to 3.2 μm sarcomere lengths. In mutant and control fibres, most of the variability (70 and 65%, respectively) in titin force enhancement is explained by the contractile stress of the fibre prior to stretch (Fig. 9). Prior to mechanical testing, fibres were activated at 2.5 μm to determine viability. A decrease in force (> 10%) between the initial activation and second activation (preceding active stretch) was observed in 30% of mutant fibres while no decrease in contractile force was observed between activations in the control fibres. This observation demonstrates that skinned mutant fibres are more sensitive to damage than control fibres. If mutant fibres are in fact more delicate than control fibres, the potential for damage in more aggressive tissue preparations (such as in myofibrils) could be greater in mutant tissue. Thus, it is plausible that titin force enhancement is not observed in mutant myofibrils largely as a result of a loss in contractile stress. Since some mutant fibres were able to generate comparable (or greater) contractile stress to control fibres, we conclude that stabilizing structures in the fibre (such as desmin and collagen) serve as compensatory mechanisms to mechanically strengthen mutant myofibrils within a skinned fibre.

Overall, this study sought to determine whether mechanical deficiencies in titin force enhancement are observed in single skinned fibres from mutant psoas muscles. We hypothesized that mutant fibres would generate less contractile stress than control fibres, corresponding with previous investigations from mutant myofibrils (Powers et al., 2016). Skinned mutant fibres generated slightly less contractile stress and comparable steady state stress following active stretch as control fibres, due to a greater concentration of collagen. By stretching single psoas fibres beyond filament overlap, we saw that titin force enhancement is overshadowed by excess collagen in skinned mutant fibres. In stretching individual fibres to lengths where collagen contributes less to the overall force, we were able to measure titin force enhancement in some, but not all, mutant fibres. We speculate that the variability in titin force enhancement in mutant fibres is due to differential effects of the mutation on fibres within a muscle. In conclusion, this study demonstrates the importance of investigating mechanical properties of muscle across hierarchical preparations. Active stiffening of sarcomeres is critical

to skeletal muscle mechanics and with variations in titin force enhancement, the collagen surrounding a muscle fibre can compensate for deficits in titin-based active stiffness.

*Limitations and Considerations*

All fibres were initially activated to measure contractile force and determine viability. Fibres were eliminated from mechanical testing when no measurable force was generated with activation. Nearly 40% of isolated mutant fibres were eliminated from mechanical testing under this criterion while less than 10% of control fibres were eliminated. This introduces a potential bias toward including the strongest mutant fibres in our samples. Sarcomere length could not be measured using laser diffraction in most mutant fibres that were tested. While the method for adjusting fibres to $L_0$ was consistent across all mutant fibres, we cannot be certain of the initial sarcomere length of every mutant fibre in this study. We were unable to pair morphological and mechanical data in the present study. While we presume that the mutant fibres with an irregular striation pattern and centralized nuclei are the weakest (and most severely affected by the mutation), we did not explicitly test this assumption.

## ACKNOWLEDGEMENTS

The authors would like to acknowledge Scott Sibole and Tim Leonard from the University of Calgary, as well as Uzma Tahir and Anthony Hessel from Northern Arizona University for contributions to this study. Statistical support was provided by Tak Fung, University of Calgary.

## COMPETING INTERESTS

No competing interests declared.

## AUTHOR CONTRIBUTIONS

Krysta Powers - data collection, analysis, interpretation, paper preparation; Venus Joumaa – mechanical data collection, analysis, interpretation and editing; Azim Jinha – data analysis, figures, editing; Eng Kuan Moo – imaging data collection, analysis and editing; Ian Curtis Smith –mechanical data collection; Kiisa Nishikawa - interpretation, editing; Walter Herzog - conceptual and experimental design, interpretation, final editing.

## FUNDING

This research was funded by Alberta Innovates Technology Futures, Natural Sciences and Engineering Research Council of Canada, Canadian Institutes of Health Research, the Canada Research Chair Programme, the Killam Trusts, the National Science Foundation (IOS-1025806 and IIP-1237878), an award from the W. M. Keck Foundation and Northern Arizona University's Technology Research Initiative Fund.

## REFERENCES


**Balogh, J., Li, Z., Paulin, D. and Arner, A.** (2003). Lower active force generation and improved fatigue resistance in skeletal muscle from desmin deficient mice. *J. Muscle Res. Cell Motil.* **24**, 453–459.

**Bartoo, M. L., Linke, Wolfgang A. and Pollack, gerald H.** (1997). Basis of passive tension and stiffness in isolated rabbit myofibrils. *Am. J. Physiol.* **273**, C266–C276.

**Bianco, P., Nagy, A., Kengyel, A., Szatmári, D., Mártonfalvi, Z., Huber, T. and Kellermayer, M. S. Z.** (2007). Interaction forces between F-actin and titin PEVK domain measured with optical tweezers. *Biophys. J.* **93**, 2102–2109.

**Boerboom, R. A., Krahn, K. N., Megens, R. T. A., van Zandvoort, M. A. M. J., Merkx, M. and Bouten, C. V. C.** (2007). High resolution imaging of collagen organisation and synthesis using a versatile collagen specific probe. *J. Struct. Biol.* **159**, 392–399.

**Buck, D., Smith, J. E., 3rd, Chung, C. S., Ono, Y., Sorimachi, H., Labeit, S. and Granzier, H. L.** (2014). Removal of immunoglobulin-like domains from titin's spring segment alters titin splicing in mouse skeletal muscle and causes myopathy. *J. Gen. Physiol.* **143**, 215–230.

**Campbell, K. S. and Moss, R. L.** (2002). History-dependent mechanical properties of permeabilized rat soleus muscle fibers. *Biophys. J.* **82**, 929–943.

**De Jaeger, D., Joumaa, V. and Herzog, W.** (2015). Intermittent stretch training of rabbit plantarflexor muscles increases soleus mass and serial sarcomere number. *J. Appl. Physiol. Bethesda Md 1985* **118**, 1467–1473.

**DuVall, M. M., Gifford, J. L., Amrein, M. and Herzog, W.** (2013). Altered mechanical properties of titin immunoglobulin domain 27 in the presence of calcium. *Eur. Biophys. J. EBJ* **42**, 301–307.

**Eastwood, A. B., Wood, D. S., Bock, K. L. and Sorenson, M. M.** (1979). Chemically skinned mammalian skeletal muscle I. The structure of skinned rabbit psoas. *Tissue Cell* **11**, 553–566.

**Edman, K. A., Elzinga, G. and Noble, M. I.** (1978). Enhancement of mechanical performance by stretch during tetanic contractions of vertebrate skeletal muscle fibres. *J. Physiol.* **281**, 139–155.

**Garvey, S. M., Rajan, C., Lerner, A. P., Frankel, W. N. and Cox, G. A.** (2002). The muscular dystrophy with myositis (mdm) mouse mutation disrupts a skeletal muscle-specific domain of titin. *Genomics* **79**, 146–149.

**Granzier, H. L. and Labeit, S.** (2004). The giant protein titin: a major player in myocardial mechanics, signaling, and disease. *Circ. Res.* **94**, 284–295.

**Greenhalgh, C., Prent, N., Green, C., Cisek, R., Major, A., Stewart, B. and Barzda, V.** (2007). Influence of semicrystalline order on the second-harmonic generation efficiency in the anisotropic bands of myocytes. *Appl. Opt.* **46**, 1852–1859.

**Heimann, P., Menke, A., Rothkegel, B. and Jockusch, H.** (1996). Overshooting production of satellite cells in murine skeletal muscle affected by the mutation "muscular dystrophy with myositis" (mdm, Chr 2). *Cell Tissue Res.* **283**, 435–441.

**Herzog, W. and Leonard, T. R.** (2002). Force enhancement following stretching of skeletal muscle: a new mechanism. *J. Exp. Biol.* **205**, 1275–1283.

**Herzog, W., Schappacher, G., DuVall, M., Leonard, T. R. and Herzog, J. A.** (2016). Residual Force Enhancement Following Eccentric Contractions: A New Mechanism Involving Titin. *Physiol. Bethesda Md* **31**, 300–312.

**Huebsch, K. A., Kudryashova, E., Wooley, C. M., Sher, R. B., Seburn, K. L., Spencer, M. J. and Cox, G. A.** (2005). Mdm muscular dystrophy: interactions with calpain 3 and a novel functional role for titin's N2A domain. *Hum. Mol. Genet.* **14**, 2801–2811.

**Joumaa, V., Rassier, D. E., Leonard, T. R. and Herzog, W.** (2008). The origin of passive force enhancement in skeletal muscle. *Am. J. Physiol. Cell Physiol.* **294**, C74–78.

**Kellermayer, M. S. and Granzier, H. L.** (1996). Calcium-dependent inhibition of in vitro thin-filament motility by native titin. *FEBS Lett.* **380**, 281–286.

**Kramerova, I., Kudryashova, E., Wu, B., Ottenheijm, C., Granzier, H. and Spencer, M. J.** (2008). Novel role of calpain-3 in the triad-associated protein complex regulating calcium release in skeletal muscle. *Hum. Mol. Genet.* **17**, 3271–3280.

**Labeit, D., Watanabe, K., Witt, C., Fujita, H., Wu, Y., Lahmers, S., Funck, T., Labeit, S. and Granzier, H.** (2003). Calcium-dependent molecular spring elements in the giant protein titin. *Proc. Natl. Acad. Sci. U. S. A.* **100**, 13716–13721.

**Leonard, T. R. and Herzog, W.** (2010). Regulation of muscle force in the absence of actin-myosin-based cross-bridge interaction. *Am. J. Physiol. Cell Physiol.* **299**, C14–20.

**Linke, W. A., Kulke, M., Li, H., Fujita-Becker, S., Neagoe, C., Manstein, D. J., Gautel, M. and Fernandez, J. M.** (2002). PEVK domain of titin: an entropic spring with actin-binding properties. *J. Struct. Biol.* **137**, 194–205.

**Lopez, M. A., Pardo, P. S., Cox, G. A. and Boriek, A. M.** (2008). Early mechanical dysfunction of the diaphragm in the muscular dystrophy with myositis (Ttnmdm) model. *Am. J. Physiol. Cell Physiol.* **295**, C1092–1102.

**Meyer, G. A. and Lieber, R. L.** (2011). Elucidation of extracellular matrix mechanics from muscle fibers and fiber bundles. *J. Biomech.* **44**, 771–773.

**Miller, M. K., Bang, M.-L., Witt, C. C., Labeit, D., Trombitas, C., Watanabe, K., Granzier, H., McElhinny, A. S., Gregorio, C. C. and Labeit, S.** (2003). The muscle ankyrin repeat proteins: CARP, ankrd2/Arpp and DARP as a family of titin filament-based stress response molecules. *J. Mol. Biol.* **333**, 951–964.

**Monroy, J. A., Powers, K. L., Gilmore, L. A., Uyeno, T. A., Lindstedt, S. L. and Nishikawa, K. C.** (2012). What is the role of titin in active muscle? *Exerc. Sport Sci. Rev.* **40**, 73–78.

**Monroy, J. A., Powers, K. L., Pace, C. M., Uyeno, T. and Nishikawa, K. C.** (2016). Effects of activation on the elastic properties of intact soleus muscles with a deletion in titin. *J. Exp. Biol.* jeb.139717.

**Moo, E. K., Fortuna, R., Sibole, S. C., Abusara, Z. and Herzog, W.** (2016). In vivo Sarcomere Lengths and Sarcomere Elongations Are Not Uniform across an Intact Muscle. *Front. Physiol.* **7**, 187.

**Nagy, A., Cacciafesta, P., Grama, L., Kengyel, A., Málnási-Csizmadia, A. and Kellermayer, M. S. Z.** (2004). Differential actin binding along the PEVK domain of skeletal muscle titin. *J. Cell Sci.* **117**, 5781–5789.

**Nishikawa, K. C., Monroy, J. A., Uyeno, T. E., Yeo, S. H., Pai, D. K. and Lindstedt, S. L.** (2012). Is titin a "winding filament"? A new twist on muscle contraction. *Proc. Biol. Sci.* **279**, 981–990.

**Palmisano, M. G., Bremner, S. N., Hornberger, T. A., Meyer, G. A., Domenighetti, A. A., Shah, S. B., Kiss, B., Kellermayer, M., Ryan, A. F. and Lieber, R. L.** (2015). Skeletal muscle intermediate filaments form a stress-transmitting and stress-signaling network. *J Cell Sci* **128**, 219–224.

**Powers, K., Schappacher-Tilp, G., Jinha, A., Leonard, T., Nishikawa, K. and Herzog, W.** (2014). Titin force is enhanced in actively stretched skeletal muscle. *J. Exp. Biol.* **217**, 3629–3636.

**Powers, K., Nishikawa, K., Joumaa, V. and Herzog, W.** (2016). Decreased force enhancement in skeletal muscle sarcomeres with a deletion in titin. *J. Exp. Biol.* **219**, 1311–1316.

**Rayment, I., Holden, H. M., Whittaker, M., Yohn, C. B., Lorenz, M., Holmes, K. C. and Milligan, R. A.** (1993). Structure of the actin-myosin complex and its implications for muscle contraction. *Science* **261**, 58–65.

**Schappacher-Tilp, G., Leonard, T., Desch, G. and Herzog, W.** (2015). A Novel Three-Filament Model of Force Generation in Eccentric Contraction of Skeletal Muscles. *PLoS ONE* **10**, e0117634.

**Sparrow, J. C. and Schöck, F.** (2009). The initial steps of myofibril assembly: integrins pave the way. *Nat. Rev. Mol. Cell Biol.* **10**, 293–298.

**Tatsumi, R., Maeda, K., Hattori, A. and Takahashi, K.** (2001). Calcium binding to an elastic portion of connectin/titin filaments. *J. Muscle Res. Cell Motil.* **22**, 149–162.

**Taylor-Burt, K. R., Monroy, J., Pace, C., Lindstedt, S. and Nishikawa, K. C.** (2015). Shiver me titin! Elucidating titin's role in shivering thermogenesis. *J. Exp. Biol.* **218**, 694–702.

**Wang, K. and Ramirez-Mitchell, R.** (1983). A network of transverse and longitudinal intermediate filaments is associated with sarcomeres of adult vertebrate skeletal muscle. *J. Cell Biol.* **96**, 562–570.

**Wang, K., McCarter, R., Wright, J., Beverly, J. and Ramirez-Mitchell, R.** (1993). Viscoelasticity of the sarcomere matrix of skeletal muscles. The titin-myosin composite filament is a dual-stage molecular spring. *Biophys. J.* **64**, 1161–1177.

**Witt, C. C., Ono, Y., Puschmann, E., McNabb, M., Wu, Y., Gotthardt, M., Witt, S. H., Haak, M., Labeit, D., Gregorio, C. C., et al.** (2004). Induction and myofibrillar targeting of CARP, and suppression of the Nkx2.5 pathway in the MDM mouse with impaired titin-based signaling. *J. Mol. Biol.* **336**, 145–154.

**Woessner, J. F.** (1961). The determination of hydroxyproline in tissue and protein samples containing small proportions of this imino acid. *Arch. Biochem. Biophys.* **93**, 440–447.

## Figures

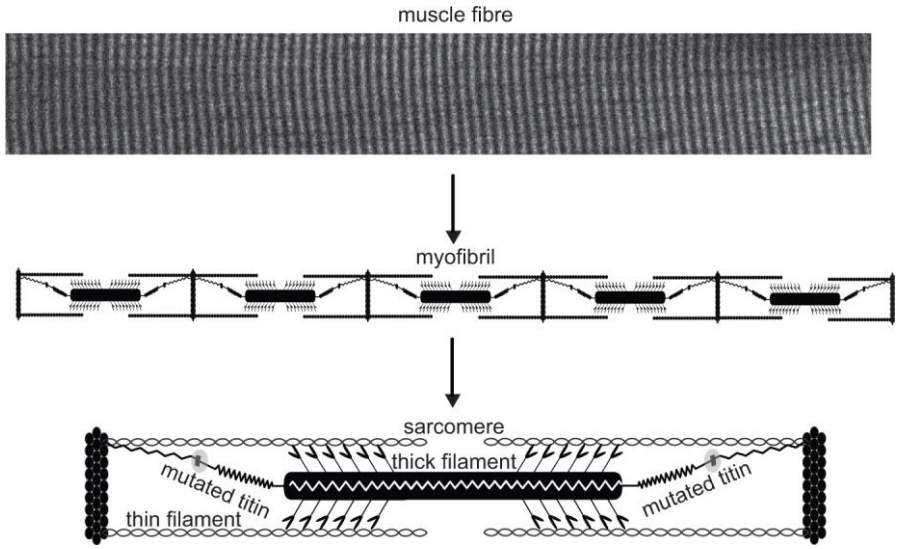


**Figure 1. Organizational hierarchy of single skinned muscle fibre.** Isolated psoas fibres from control and titin-mutant mice were mechanically tested. A segment of a single muscle fibre from control psoas, imaged using second harmonic generation technique, (top) illustrates the hierarchy of muscle organization. Myofibrils in parallel make up a muscle fibre. Each myofibril is made up of sarcomeres in series (middle). The mutation used, *muscular dystrophy with myositis*, results in an amino acid deletion in the titin protein within the sarcomere. The mutated region of titin in the sarcomere is circled in gray (bottom). In this study, we investigated the effect of a titin mutation on the mechanics of single fibres.

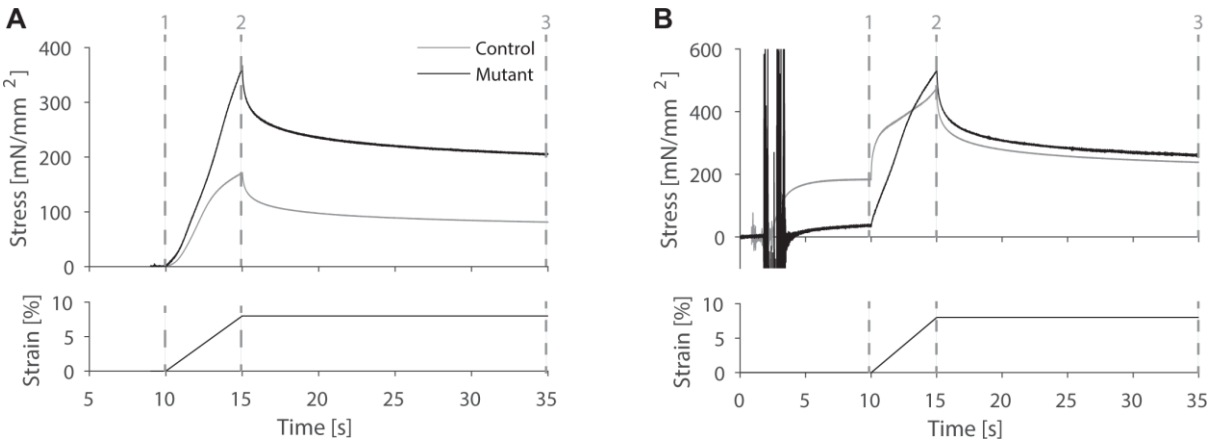


**Figure 2. Examples of the stretch protocol in single skinned fibres.** Single fibres from control (gray) and mutant (black) mice were passively (A) and actively (B) stretched by a strain of 8% of the total fibre length from an average initial sarcomere length of 2.5 μm to a final average sarcomere length of 5.2 μm. Long stretches were implemented to observe stress ($mN/mm^2$) in the absence of cross-bridges in actively stretched fibres (B). Dotted lines indicate start of stretch (1), end of stretch (2) and steady state force (3). In actively stretched fibres (B), activation preceded start of stretch.

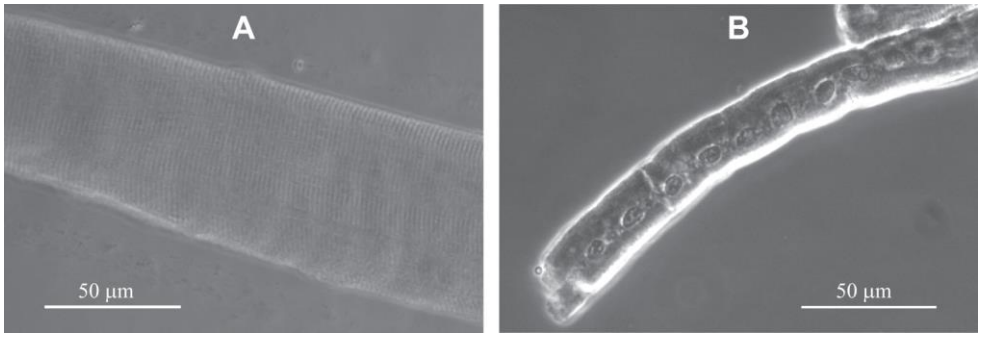


**Figure 3. Example psoas fibres from control and mutant mice.** Single fibres were isolated and imaged under a light microscope at 50X magnification. Control fibres (A) were larger in diameter (*n*, mean ± standard deviation) (*50*, 52 µm ± 10) than mutant fibres (B) (*38*, 20 µm ± 4) ($p < 0.05$, *t*-test) and were consistently cylindrical, with a clear striation pattern. Mutant fibres (B) had variable striation patterns, shape and morphology.

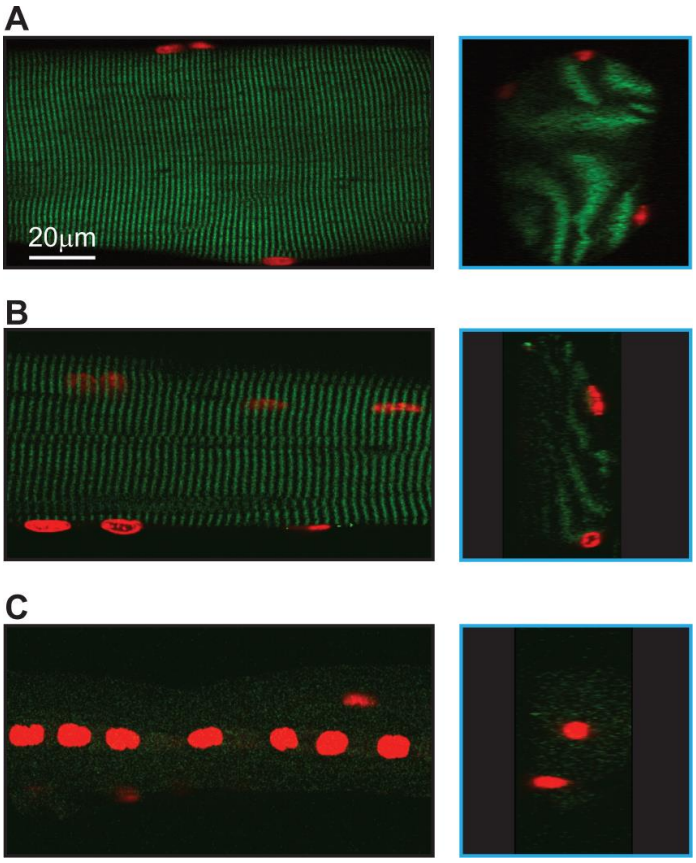


**Figure 4. Orthogonal view of three-dimensional images exhibits the differences in striation patterns and arrangement of nuclei between exemplar control (A) and mutant (B, C) psoas fibres.** The xy-plane is perpendicular to the objective axis and parallel to the fibre long axis. Views from the xz-plane and yz-plane are shown in orange and blue windows, respectively. Control fibres (A) displayed a regular striation pattern (green) with multiple nuclei (red) located on the fibre surface. Mutant fibres (B, C) showed two morphological states. One subgroup of mutant fibres displayed a regular striation pattern with multiple nuclei along the periphery of the fibre (B). A second subgroup of mutant fibres showed a diminished striation pattern with nuclei residing within the fibre and aligned in series along the longitudinal axis of the fibre (C).

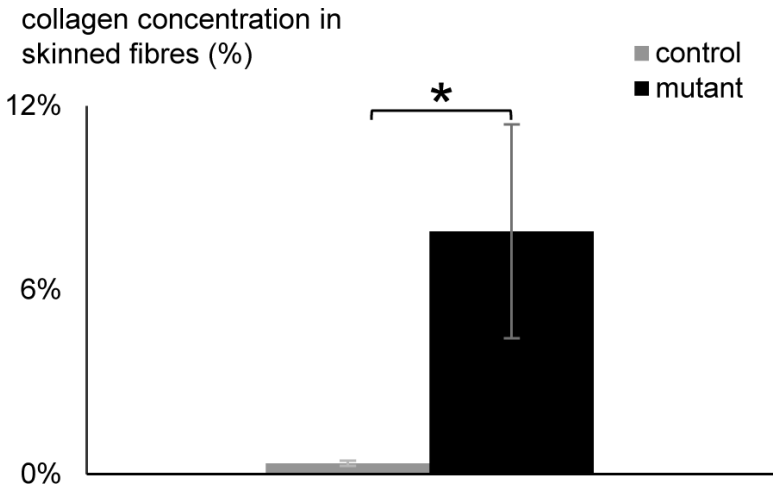


**Figure 5. Mutant fibres contain a greater concentration of collagen than control fibres.** Collagen concentration (%), calculated based on measured mass of hydroxyproline (μg), was greater in skinned mutant fibres (*n*, mean ± standard deviation; *5*, 7.9 ± 3.5%) than control fibres (*6*, 0.3 ± .01%) (p = 0.004, *Mann-Whitney U*, significance indicated by *).

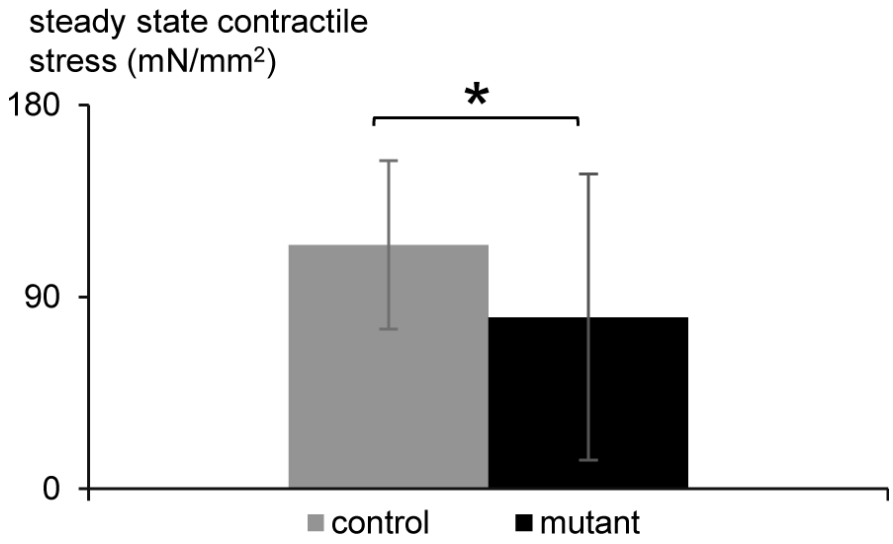


**Figure 6. Control fibres generate higher steady state contractile stress than mutant fibres.** Steady state contractile stress (mN/mm$^2$) of single skinned fibres from control and mutant mouse psoas activated (pCa 4.2) at 2.5 μm sarcomere lengths. Steady state contractile stress (*n*, mean ± standard deviation) of control fibres (*35*, 115 ± 40 mN/mm$^2$) is greater than mutant fibres (*31*, 81 ± 67 mN/mm$^2$) (p = 0.017, *t-test*, significance indicated by *). Mutant fibres had higher contractile stress variability than control fibres (p = 0.049, *Levene's test*).

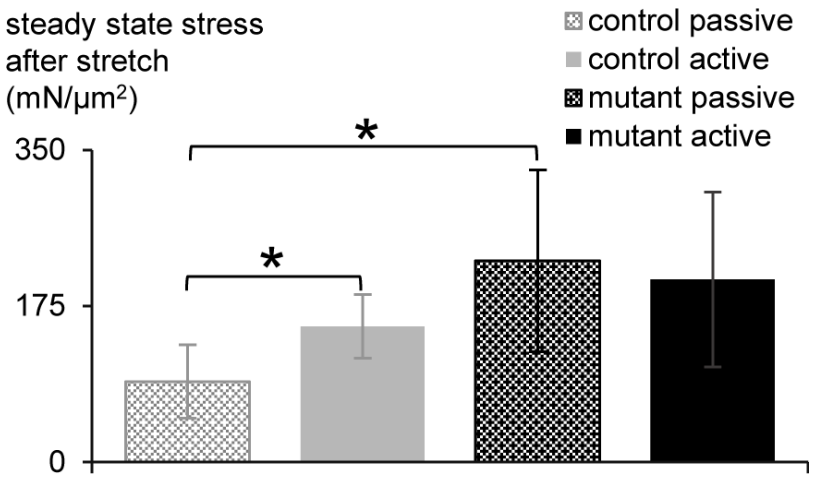


**Figure 7. Passive and active steady-state stress of single fibres following stretch to 5.2 µm average sarcomere lengths.** Average passive (patterned) and active (solid) steady state stress ($mN/mm^2$) of control (gray) and mutant (black) fibres stretched from average sarcomere lengths of 2.5 µm to 5.2 µm. Control fibres had less passive stress (*n*, mean ± standard deviation; *10*, 90 ± 41 $mN/mm^2$) than passive mutant fibres (*11*, 226 ± 101 $mN/mm^2$) ($p$ = 0.0009*)*. Steady state stress in actively stretched control (*15*, 152 ± 36 $mN/mm^2$) and mutant fibres (*18*, 204 ± 98 $mN/mm^2$) did not differ ($p$ = 0.0596). The active steady state stress in control fibres was greater than the passive steady state stress while passive and active steady state stress did not differ in mutant fibres ($p$ = 0.0005 and $p$ = 0.5872 respectively). Bonferroni corrected p-value is 0.0083 for considering statistical significance (indicated by *) for pairwise comparisons.

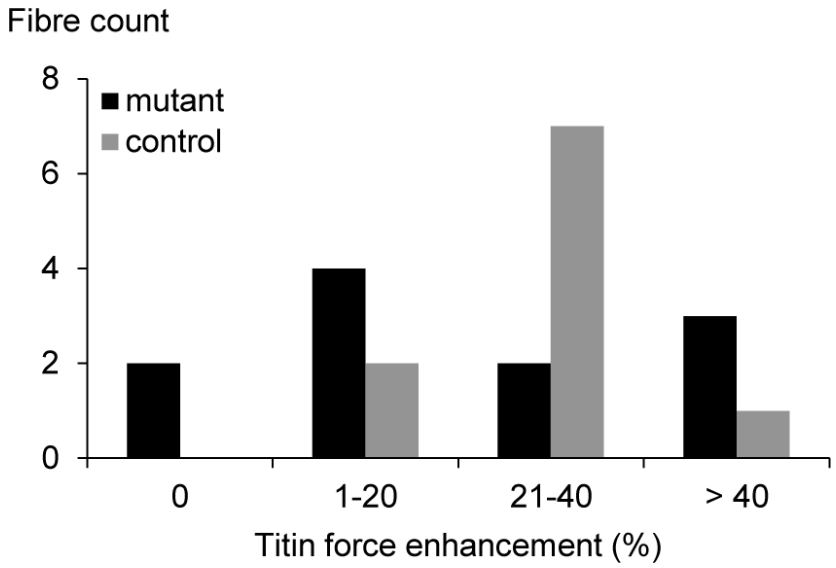


**Figure 8. Histogram of calculated titin force enhancement in control and mutant fibres.** Titin force enhancement, defined as the % of stress remaining in an actively stretched fibre after subtracting the passive stress and contractile stress at (average sarcomere length = 3.2 μm). The histogram shows fibre count for indicated bins of titin force enhancement (%) in mutant (black, n = 11) and control (gray, n = 10) fibres. The percent titin force enhancement did not differ between mutant 22 ± 18% (mean ± standard deviation) and control fibres 28 ± 9% ($p$ = 0.557, Mann-Whitney U. Mutant fibres showed higher variability in titin force enhancement than control fibres ($p$ = 0.011, *Levene's*). The first bin (designated as 0) only contains fibres with no calculated titin force enhancement. Most control fibres had 21-40% titin force enhancement. Mutant fibres generated variable magnitudes of titin force enhancement, with 2 mutant fibres having no titin force enhancement.

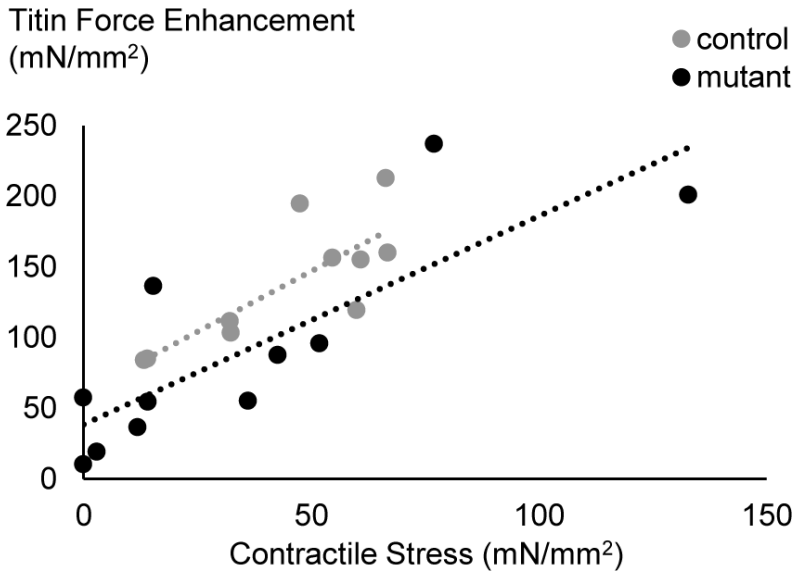


**Figure 9. The magnitude of titin force enhancement correlates to the initial contractile stress of control and mutant fibres.** The magnitude of titin force enhancement (mN/mm$^2$) is correlated to contractile stress (mN/mm$^2$) for control (gray, n =10) and mutant (black, n =11) fibres activated at 2.5 µm and then actively stretched to 3.2 µm average sarcomere lengths ($p$ = 0.005 and $p$ = 0.001 respectively). The magnitude of contractile stress explains 65% of the variability in titin force enhancement in control fibres (*Spearman's correlation coefficient* = 0.806, $R^2$ = 0.649). Contractile stress (mN/mm$^2$) explains 70% of the variability in titin force enhancement in mutant fibres (*Spearman's correlation coefficient* = 0.836; $R^2$ = 0.699). Tread lines depicting the relationship between titin force enhancement and contractile stress are included for mutant (black) and control (gray) fibres.